minerals

MDPI

Article

Stimulation of Biomethane Productivity in Anaerobic Digestion Using Electro-Conductive Carbon-Nanotube Hollow-Fiber Media

Seongmin Yang [1], Seungyeob Han [1], Yeo-Myeong Yun [2,*] and Seoktae Kang [1,*]

[1] Department of Civil and Environmental Engineering, KAIST, 291 Daehak-ro, Yuseong-gu, Daejeon 34141, Korea; yssm0303@kaist.ac.kr (S.Y.); sksm91@gmail.com (S.H.)
[2] Department of Environmental Engineering, Chungbuk National University, Cheongju 28644, Korea
* Correspondence: ymyun@chungbuk.ac.kr (Y.-M.Y.); stkang@kaist.ac.kr (S.K.); Tel.: +82-43-261-2466 (Y.-M.Y.); +82-42-350-3635 (S.K.); Fax: +82-43-264-2465 (Y.-M.Y.); +82-42-350-3610 (S.K.)

Abstract: The production of biogas was promoted via direct interspecies electron transfer (DIET) by employing electro-conductive carbon-nanotube hollow-fiber media (CHM) in anaerobic digestion. Experimental results showed a positive effect of CHM presence on CH_4 productivity with 34% higher CH_4 production rate than that of in the presence of non-electroconductive polymeric hollow fiber media. An increased CH_4 production rate was due to the shift in the microbiome with more abundant *Pelobacter* (10.0%), *Geobacter* (6.9%), and *Methanosaeta* (15.7%), which play key roles in promoting CH_4 production via syntrophic metabolism associated with DIET. Microscopic morphology analysis, using confocal laser scanning microscopy and scanning electron microscopy, exhibited that several living cells were attached with electro-conductive *pili* on the CHM surface, thereby facilitated electron transport between microbial cells.

Keywords: anaerobic digestion; carbon nanotube hollow-fiber media; direct interspecies electron transfer; *Pelobacter*; *Methanosaeta*

Citation: Yang, S.; Han, S.; Yun, Y.-M.; Kang, S. Stimulation of Biomethane Productivity in Anaerobic Digestion Using Electro-Conductive Carbon-Nanotube Hollow-Fiber Media. *Minerals* **2021**, *11*, 179. https://doi.org/10.3390/min11020179

Academic Editor: Carolina Cruz Viggi
Received: 13 January 2021
Accepted: 4 February 2021
Published: 8 February 2021

1. Introduction

Increasing global concern regarding waste management and energy security is driving the technological development related to the waste-to-energy concept. Anaerobic digestion (AD) is a well-established and mature technology that not only stabilizes organic wastes, but also produces biogas, which is a mixture of CH_4 and CO_2 [1,2]. Currently, 132,000 AD plants are utilized globally, and the biogas market size is projected to reach USD 32 billion by 2027 [3].

Anaerobic digestion is strongly dependent on the mutualistic and syntrophic interactions of the anaerobic microbiome to break down organic compounds via a series of biological processes, i.e., hydrolysis, acidogenesis, acetogenesis, and methanogenesis [4,5]. During hydrolysis, large organic molecules are first decomposed to soluble monomers by hydrolytic bacteria and are subsequently converted into acetic acid, H_2, and CO_2 during acidogenesis and acetogenesis. Finally, methanogenic archaea produce CH_4 from acetic acid and H_2.

Process instability due to the complex AD food web is a common operational issue hampering the AD technology from being widely adopted. A major factor affecting the performance and stability of AD systems is the relatively slow syntrophic metabolism between syntrophic bacteria (i.e., H_2 production) and methanogenic archaea (i.e., H_2 consumption). It is believed that the main interaction between these two types of microorganisms during AD is based on interspecies electron transfer (IET), in which hydrogen serves as an electron carrier [6,7].

Syntrophic bacteria degrade a variety of organic compounds and produce acetate and H_2 through energetically unfavorable reactions. To make this reaction thermodynamically

exergonic, methanogenic archaea always play a crucial role in regulating the H_2 level. The fluctuation of the H_2 partial pressure is critical for the syntrophic relation of the IET. This fluctuation often causes accumulation of organic acids, and as a result, the reactor can fail. [8,9].

Recent studies have introduced direct interspecies electron transfer (DIET) from cell to cell between electroactive bacteria and methanogenic archaea partners through electrically conductive *pili* and *c-type* cytochrome [10,11]. DIET is more efficient than IET because it does not require multiple enzymatic steps for producing H_2 as an electron carrier and generation and diffusion of metabolites [12].

Several studies have further demonstrated that the CH_4 production improvement in AD is amended with the addition of a variety of conductive materials that can serve as electrical conduits to facilitate DIET. The vast majority of DIET studies have supplemented carbon-based conductive materials of various types of substrates in AD [13]; however, there is no clear evidence of DIET in the mixed culture. Furthermore, these supplements are easily washed out during continuous operation [6]. Carbon-nanotube hollow-fiber media (CHM) provide a large surface area where multiple microorganisms can be immobilized. In addition, CHM have increased stability and electrical conductivity; hence, they are suitable as conductive material in AD [14,15].

In this study, we evaluated the effect of CHM on biogas productivity during continuous AD. Reactor 1 (R1) included CHM; Reactor 2 (R2)—used as control—included polymeric hollow-fiber media (PHM), i.e., insulative material with similar biomass retention properties. To visualize the influence of CHM on AD, we utilized scanning electron microscopy (SEM) and confocal laser scanning microscopy (CLSM). Both R1 and R2 microbiomes were further analyzed via 16S rRNA-based next-generation sequencing (NGS) to reveal more comprehensive insights into the microbial behavior related to DIET.

2. Materials and Methods

2.1. Preparation of Seed Sludge and Feedstock

The seed sludge was collected from an up-flow anaerobic sludge blanket at a local brewery wastewater treatment plant located in Cheong-Ju, Korea. This inoculum was acclimated at 35 °C under anaerobic conditions for 14 days to remove residual compounds. The total solids (TS), volatile solids (VS), alkalinity, and pH of the seed sludge were 7.2 g/L, 3.6 g/L, 3.3 g $CaCO_3$/L, and 7.0, respectively.

After the successful preparation of the microbe growth medium, the BA medium was prepared using the following (per liter): $NaHCO_3$, 4.12 g; yeast extract, 0.56 g; KH_2PO_4, 219.4 mg; NH_4Cl, 955.4 mg; $FeCl_2$, 37.8 mg; resazurin solution, 1 mL; and trace element solution, 0.1 mL. The resazurin solution composition was as follows: resazurin, 0.5 mg/L; $MgCl_2 \cdot 6H_2O$, 10 mg/L; and $CaCl_2$, 5 mg/L. The composition of trace element solution comprised (per liter) the following: $Na_2MoO_4 \cdot 4H_2O$, 0.1 mg; $MgCl_2 \cdot 6H_2O$, 1000 mg; $CaCl_2$, 750 mg; H_3BO_3, 0.5 mg; $MnCl_2 \cdot 4H_2O$, 5 mg; $ZnCl_2$, 0.5 mg; $CuCl_2$, 0.3 mg; $NiCl_2 \cdot 6H_2O$, 0.5 mg; $CoCl_2 \cdot 2H_2O$, 5 mg; Na_2SeO_3, 0.5 mg; EDTA, 5 mg; and $AlCl_3$, 0.5 mg. Ethanol was used as a carbon source.

2.2. Preparation of Carbon-Nanotube Hollow-Fiber Media and Polymeric Hollow Fiber Media

Carbon-nanotube hollow-fiber media were fabricated using the wet spinning method with thermal calcination [16]. Multi-wall carbon nanotubes (MWCNTs; Cheap Tubes Inc., Cambridgeport, VT, USA) and polyvinyl butyral (PVB) solution were dispersed in 17 g of N-Methyl-2-pyrrolidone (NMP) and sonicated for 30 min. The prepared spinning solution was extruded into deionized water through an outer stainless-steel capillary, and then, the extruded hollow structure was calcined at 350 °C for 1 h in an Ar environment to remove PVB from the carbon nanotube media. The pore size, surface area, and conductivity of the CHM were 13.76 nm, 77.81 m^2/g, and 57.5 s/cm, respectively. A polymeric hollow-fiber media (PVDF, Synopex, Hwaseong-si, Korea) was used as a non-conductive hollow-fiber structure for comparison.

2.3. Experiments

The anaerobic reactor volume was 250 mL, while the working volume was 200 mL. A magnetic stirrer stirred the reactors at 150 rpm, while the outlet and inlet ports of the feed were attached to the top of the reactor. Furthermore, the gas collector was connected to a gas outlet line. A water bath was used as temperature controller at 37 ± 2 °C. Seed sludge was inoculated into 100 mL of the reactor with 100 mL of deionized water. The initial pH was adjusted to 7.0 for optimum reactor operation. After the injection, the reactors were flushed with N_2 gas for 3 min to remove the oxygen. Twenty mL of feedstock was prepared at a concentration of 0.5 g chemical oxygen demand (COD)/L, with 10 days hydraulic retention time (HRT) and 0.5 g COD/L/day organic loading rate (OLR). The reactor was operated for 104 days in a sequencing batch mode (0.5 h of feeding, 22.5 h of reaction, and 1.0 h of settling) to prevent washout of the CHMs. CHM and PHM (1400 mg each) were injected into R1 and R2, respectively. The organic loading rate was 0.5 g COD/L/day, while it was increased stepwise to 4 g COD/L after stabilizing the performance in each step. On day 24, CHM and PHM were supplemented to R1 and R2, respectively.

2.4. Sample Analysis

Total suspended solids (TSS), volatile suspended solids (VSS), and alkalinity were analyzed following the Standard Methods for the Examination of Water and Wastewater (APHA, 1998) [17]. Soluble COD was determined using a kit (Humas, Daejeon, Korea) after particles were filtered using 0.45 µm PVDF filters (Advantec, Tokyo, USA). Biogas volume was monitored every 24 h. A gas chromatograph analyzed the biogas composition with a thermal conductivity detector (GC-TCD 580, Gow-Mac series, Bethlehem, USA). A stainless steel column packed with molecular sieve (80/100 mesh) was used, and nitrogen gas served as the mobile phase. The injector, detector, and column temperatures were 60, 80, and 80 °C, respectively. High-performance liquid chromatography (HPLC, Shimadzu Scientific instruments, MD) was used for the analysis of organic acids with an ultraviolet (210 nm) detector (SPD-10A, Shimadzu) and Aminex HPX-87H column 300 mm × 7.8 mm (Bio-Rad, California, USA). Microorganisms attached to CHM or PHM were observed via scanning electron microscopy (SEM) and confocal laser scanning microscopy (CLSM) (Carl Zeiss, Jena, Germany).

2.5. Microbial Community Analysis

DNA samples were extracted from R1, R2, and seed sludge using an Ultraclean soil DNA kit and were subsequently purified using an Ultraclean Microbial DNA Isolation Kit (Mo Bio Laboratory Inc., Carlsbad, CA, USA) according to the manufacturer's instructions. After DNA extraction and purification, the variable region (V3-V4) of the 16S rRNA gene was amplified using universal primer sets 519F (5'-CCTACGGGNGGCWGCAG-3') and 806R (5'-GACTACHVGGGTATCTAATCC-3'). According to the manufacturer's instructions from a commercial sequencing facility, high-throughput sequencing was performed using an Illumina MiSeq platform (Illumina, San Diego, CA, USA) (Macrogen, Seoul, Korea). The raw paired-end reads from Illumina Miseq were subsequently analyzed with the software QIIME for pre-processing (quality-adjustment, barcode split), identification of operational taxonomic units (OTUs), community diversity indices (e.g., CHAO1, Shannon, and Simpson), and taxonomic assignment.

3. Results and Discussion

3.1. Effect of CHM on AD Performance

Figure 1 shows the daily variation of the CH_4 production rate (MPR) and COD removal efficiency of R1 and R2. As the initial OLR was 0.5 g COD/L/day, an MPR of 135 ± 10 mL/L/day in both R1 and R2 was detected; however, it subsequently dropped and stabilized at 70 ± 6 mL/L/day with approximately 63% COD removal efficiency beyond that point. This was mainly due to the excess CH_4 being temporarily produced from leftover COD in the seed sludge during the first period (days 1–11). As the OLR

increased to 1 g COD/L/day (days 12–24), the MPR of both reactors increased, reaching 137 ± 6 mL/L/day, and the average COD removal efficiency gradually increased to 72% in both reactors.

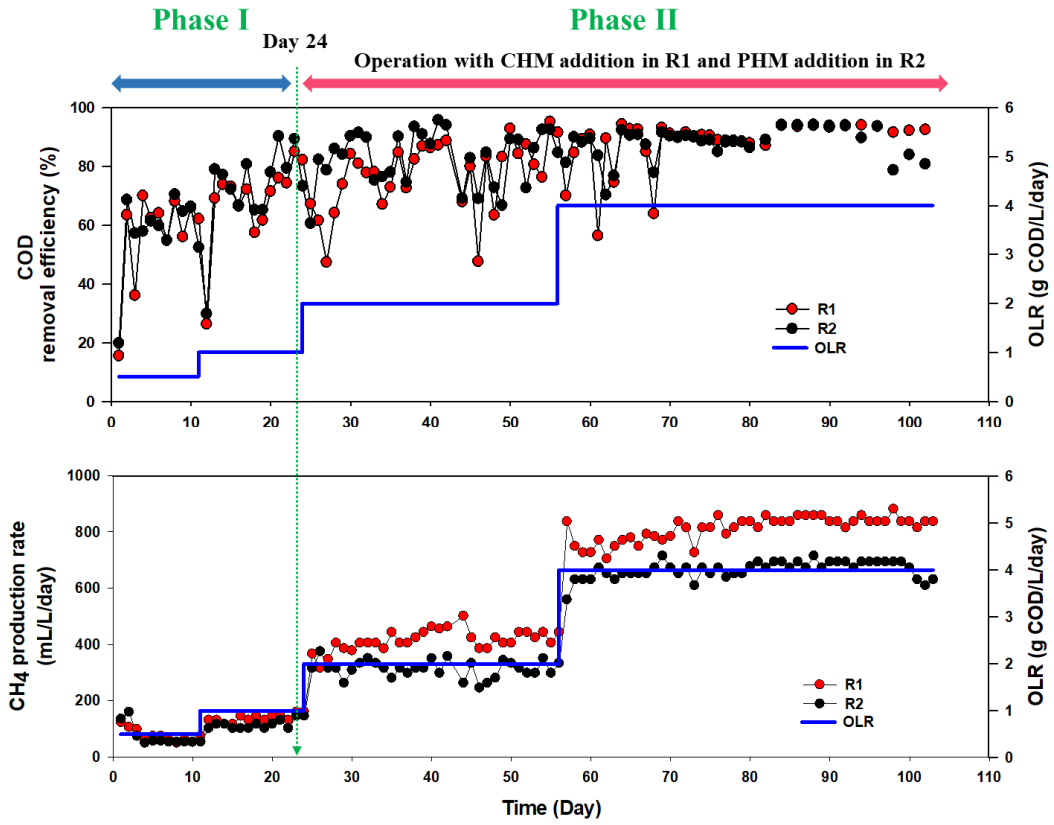

Figure 1. Daily variation of chemical oxygen demand (COD) removal efficiency and CH_4 production rate in R1 and R2 at various organic loading rates.

On day 24, CHM and PHM were supplemented to R1 and R2, respectively, and OLR further increased to 2 g COD/L/day. In both reactors, COD removal efficiency was not significantly different, while it was found that CHM addition to R1 led to a gradual MPR increase, reaching 30% higher MPR (426 ± 39 mL/L/day) compared to R2 after PHM addition (321 ± 50 mL/L/day). Organic acids remained below 183 mg COD/L in both reactors, attributed mainly to the acetate (77–79%) and lactate (21–23%) in both reactors (Figure 2). Bicarbonate alkalinity (>5000 mg $CaCO_3$/L) was high enough to prevent significant pH fluctuations, resulting in pH of approximately 7.2–7.4 in both reactors. The positive effect of CHM on AD increased with the increase in OLR to 4 g/L/day (days 59–104). The MPR was 839 ± 15 mL/L/day in R1 and 675 ± 24 mL/L/day in R2. Under these conditions, the CH_4 content in biogas was 68% in R1 and 60% in R2. A gradual reduction of total organic acid with no acetic acid was detected in the effluent of R1, indicating that electrical advance stimulates methanogen conversion from acetate to methane [18]. Meanwhile, the total organic acid content of R2 was the same as that corresponding to an OLR of 2 g COD/L/day.

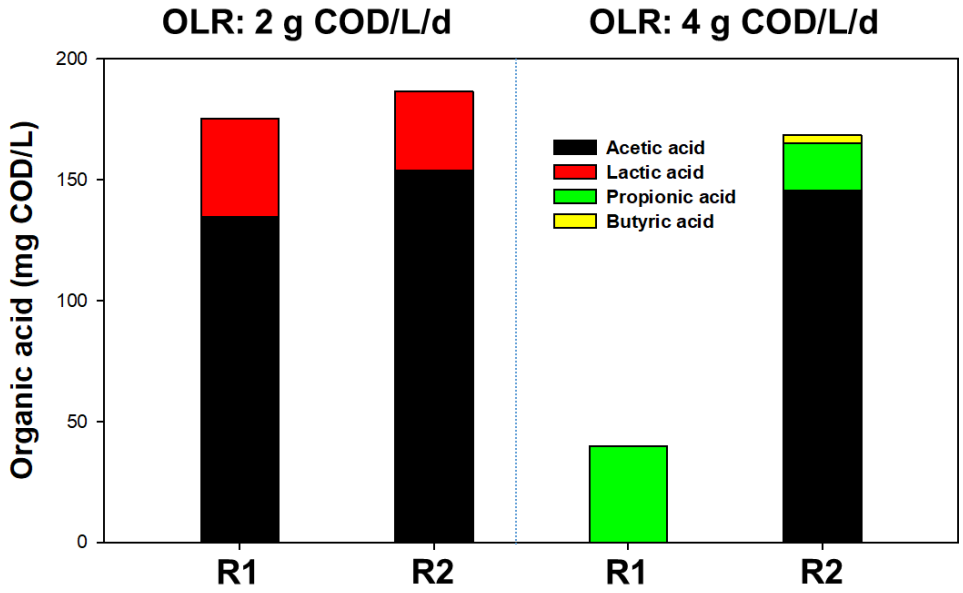

Figure 2. The performance of the organic acid at the steady-state of the reactor with polymeric hollow-fiber media (PHM) and carbon-nanotube hollow-fiber media (CHM).

3.2. Change in Taxonomic Distribution of the Microorganisms

To reveal the changes in the AD microbiome as a result of performance enhancement by CHM (R1) and PHM (R2) addition, mixed liquor samples from seed sludge (day 0) and samples at day 90 (R1 and R2) were analyzed via NGS. Log-shaped rarefaction curves of three samples at a similarity of 97% indicate that the sequences were reliable (data not shown). A total of 166,492 high-quality sequence reads were generated and classified into 358 operational taxonomic units (OTUs), as shown in Table 1. The Shannon index and CHAO1 provide species richness and evenness among all microbial communities [19]. The diversity and richness of both R1 and R2 were lower than those of seed sludge.

Table 1. Analytical results of the microorganism gene libraries obtained from NGS.

Sample	Read Count	OTUs	Chao1	Shannon
Seed sludge	45,917	158	158.75	3.69
R1	58,396	103	108.83	2.30
R2	62,178	97	109.21	2.12

The kingdom, class, and genus levels of relative microbial abundance were categorized, and minorities of OTUs (i.e., <1% of relative abundance) in the samples were classified as "Others."

As shown in Figure 3a, a gradual increase in OTUs associated with archaea in R1 and R2 was detected (18.8% at R1 and 25.4% at R2), and the archaea/bacteria (A/B) ratio was 0.23 (R1) and 0.34 (R2). Meanwhile, the abundance of archaea in the seed sludge was only 5.2%, corresponding to an A/B ratio of 0.05. This result indicates that the archaeal community was developed in both reactors. Regueiro et al. [20] reported that the quantitative percentage of A/B ratio in AD varies from to 0.1–0.7. In addition, given that higher MPR in R1 compared to R2 was associated with lower A/B ratio, the effect of CHM on the syntrophic metabolic pathway associated with DIET in R1 may be positive.

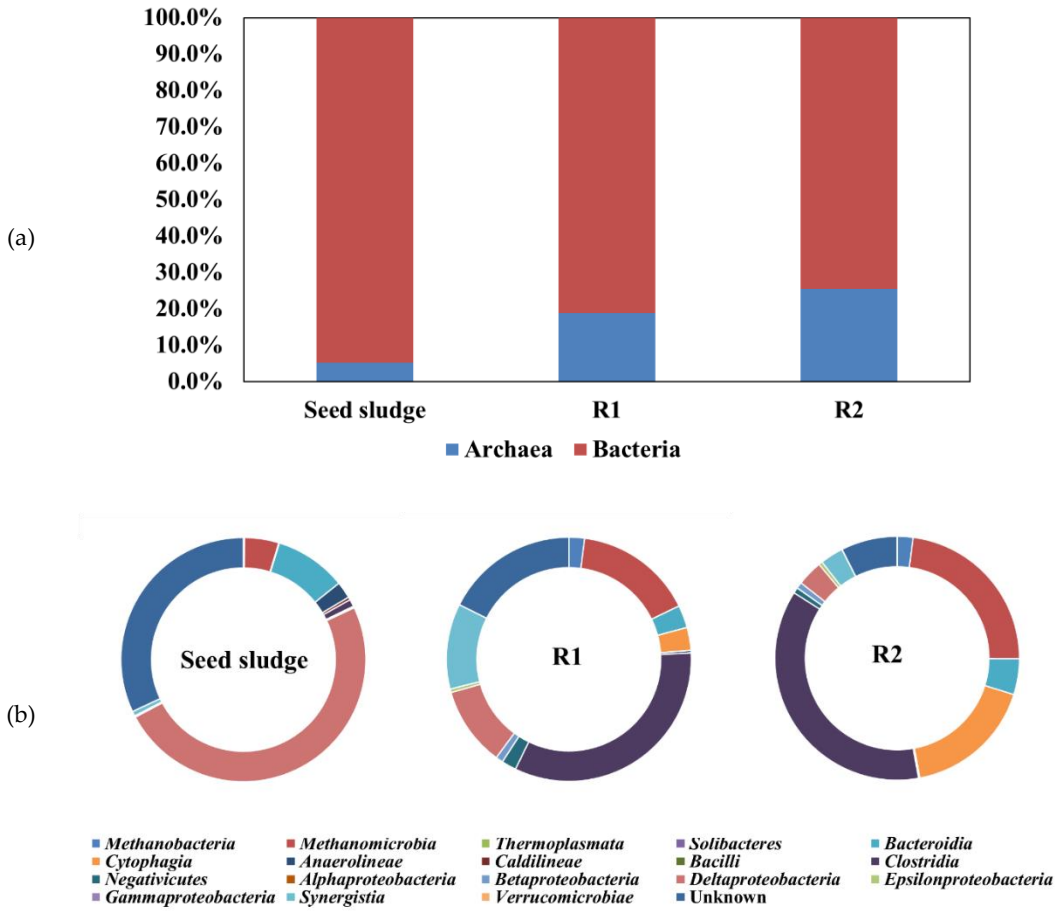

Figure 3. Relative abundances of microorganisms of seed sludge, R1 (with CHM), and R2 (with PHM) at (**a**) kingdom level and (**b**) class level (Seed sludge: the sample was taken from the seed sludge; R1 and R2: the samples were taken at the end of operation).

The distribution of microbial abundance at the class level illustrated in Figure 3b shows that the predominant microbial community in the seed sludge was *Deltaproteobacteria* (49.2%) and *Bacteroides* (9.5%). However, decreased amounts of *Deltaproteobacteria* were observed, accounting for 10.5% and 3.4% in R1 and R2, respectively, while increased abundance of *Clostridia* and *Methanomicrobia* was found in both R1 (33.0% and 15.7%) and R2 (36.8% and 23.0%). *Clostridia* are among the most frequently observed acid-producing bacteria, and *Methanomicrobia* are known as CH_4 producing archaea [21,22]. Hu et al. [23] verified that these two types of microorganisms promote synergistic CH_4 production through carbohydrate degradation, production of organic acids and H_2, and methanogenesis. Other class members, including *Synergistia* (11.3% in R1) and *Cytophagia* (17.2% in R2), were also observed with high abundance in both R1 and R2.

The distributions of the microbiome at the genus level are shown in Figure 4. *Syntrophobacter* (44.8%) was found to be predominant in the seed sludge, followed by *Thermodesulfovibrio* (20.4%), *Methanosaeta* (4.4%), *Paludibacter* (4.1%), *Marinilabilia* (3.6%), *Geobacter* (2.8%), and *Levilinea* (1.5%). *Syntrophobacter* and *Thermodesulfovibrio* are known to syntrophically oxidize organic acids and can induce IET to provide H_2 to methanogens [10]; however, their abundance decreased as the operation progressed while giving way to newly emerged bacterial microbiomes in both R1 and R2. *Lutispora* and *Methanosaeta* became the main members, whose total amount accounted for 47.1% and 57.7% in R1 and R2, respectively. Other genera, including *Aminiphilus*, *Pelobacter*, *Geobacter*, *Parapedobacter*, and *Methanobrevibacter*, also became more abundant in both R1 and R2.

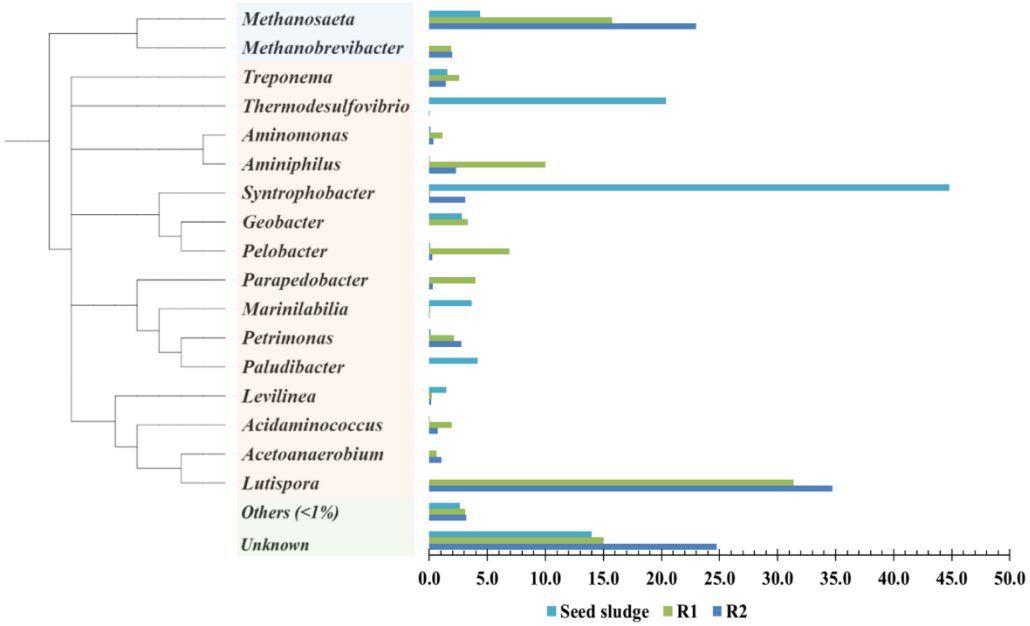

Figure 4. The relative abundances of microorganisms of seed sludge, R1 (with CHM), and R2 (with PHM) at genus level (Seed sludge: the sample was taken from the seed sludge; R1 and R2: the samples were taken at the end of operation). Genera with less than 1% abundances were classified into others.

Regarding the influence of CHM in AD (R1 vs. R2), a different dominant microbiome was a crucial finding. The abundances of *Aminiphilus*, *Pelobacter*, and *Geobacter* were significantly higher in R1 than in R2, accounting for 10.0%, 6.9%, and 3.3% in R1 and 2.3%, 0.3%, and 0.0% in R2, respectively. *Pelobacter* and *Geobacter* seemed to be key microorganisms for DIET in R1. These are known as electroactive bacteria and have often been observed in the DIET system in AD [24,25]. *Pelobacter,* a syntrophic bacterium that oxidizes ethanol to acetic acid, is likely to promote DIET in the presence of CHM in R1, thereby enhancing MPR with a high abundance of *Methanosaeta* (15.7%) [26]. *Methanosaeta* is a well-known electron-accepting microorganism that can directly convert CO_2 to CH_4 using the DIET pathway [27]. Increased abundance of *Aminiphilus* in R1 was related to propionate oxidizing syntrophic association [28]. This result is in agreement with a previous study showing that propionate-oxidizing bacteria are also likely to be involved in DIET [6].

3.3. Effect of CHM on Direct Interspecies Electron Transfer

Many studies have employed various types of conductive materials to stimulate methanogenesis via DIET in AD [6,14,27,29]. They demonstrated that conductive materials could be the conduit for electron transfer between microorganisms that replaced the IET pathway. DIET has the advantage of faster electron transfer than IET, which is the H_2 diffusion pathway. DIET pathway has been established with various conductive materials. Magnetite was proven to promote the growth of syntrophic bacteria [12]. In addition, the vast majority of studies have used carbon materials as a conductive material to promote DIET in AD. It has been revealed that the addition of activated carbon stimulated DIET in the AD of various types of substrates [13]. Zhao et al. (2016) also observed that the biogas production rate increased in the presence of biochar [10]. However, the addition of those materials into AD is not economically feasible because those may easily wash out during long-term continuous operation. In contrast, CHM can provide a practical solution to this challenge. In addition, the large surface area (77.81 m^2/g) of CHM was beneficial for enriching electroactive bacteria and methanogens on the surface to promote DIET. However, previous studies have reported that carbon nanotubes (CNTs) have a physical cytotoxic effect on microbes, which can affect microbial community activity and diversity. This toxic effect was determined by the physicochemical characteristics of CNTs (e.g., single-wall

or multi-wall) [30,31]. In order to verify the toxic effect of CHM on the microbiome in R1, CLSM was analyzed. Figure 5a shows several living cells of microorganisms (blue color) densely attached to the surface of the CHM, indicating lack of noticeable microbial toxic effect. In addition, as shown in Figure 5b, microbiomes with *pili* were attached to the CHM surface, indicating that the CHM played a key role as electrical conduits facilitating electronic connections between microbial cells, leading to a higher MPR in R1 compared to R2, where non-conductive hollow fiber type media were added.

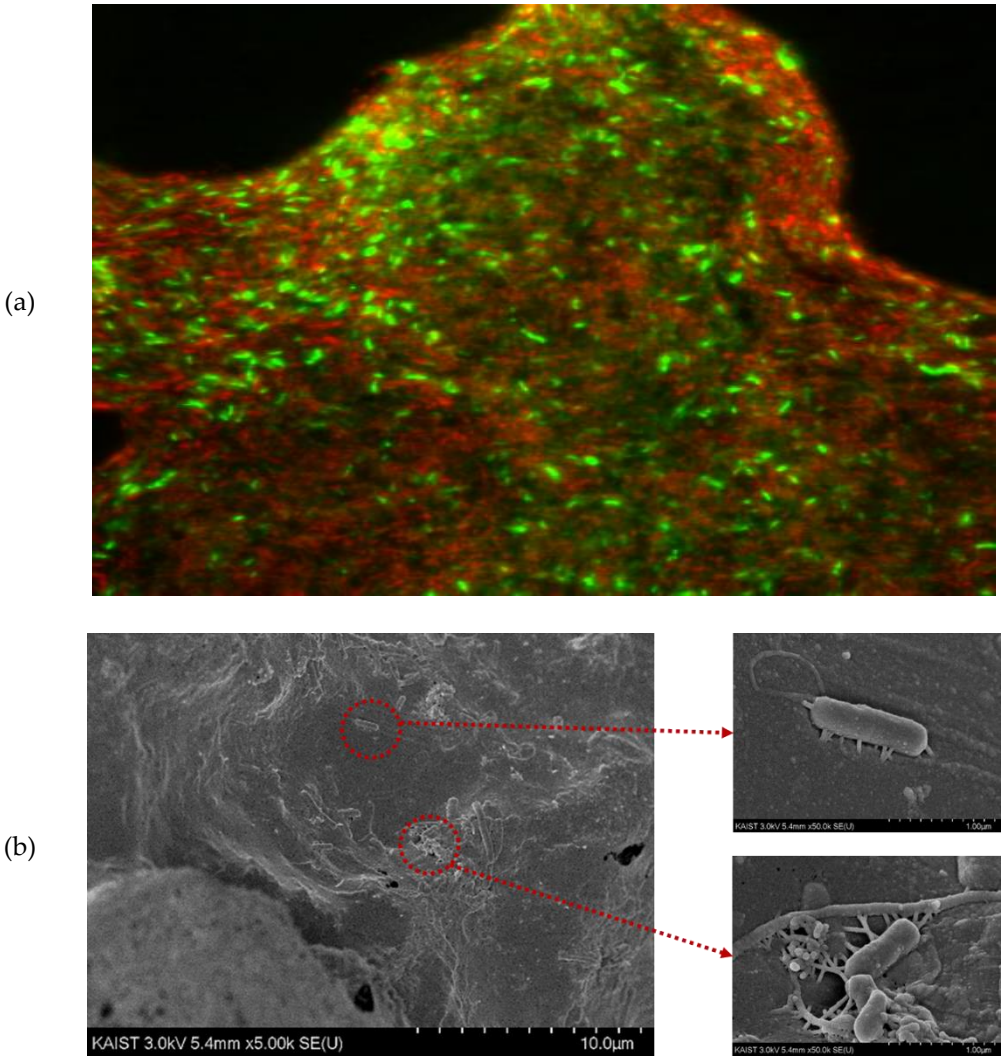

Figure 5. (**a**) The confocal laser scanning microscopy (CLSM) and (**b**) scanning electron microscopy (SEM)images of biofilm attached to the surface of CHM taken from R1 at the end of operation.

4. Conclusions

In this study, a higher CH_4 production rate associated with lower archaea/bacteria ratio showed that carbon-nanotube hollow-fiber media (CHM) have a positive effect on the metabolic pathway of anaerobic digestion (AD). This was further verified by the changed microbiomes (*Pelobacter*, *Geobacter,* and *Methanosaeta*) associated with lower concentration of organic acids, making syntrophic metabolism thermodynamically exergonic. SEM and CLSM images revealed the dense attachment of microorganisms on the CHM surface with *pili*. This study provides evidence of direct interspecies electron transfer (DIET) and utilization of CHM under anaerobic conditions to enhance CH_4 production and may elucidate the microbial DIET of AD.

Author Contributions: Formal analysis and writing—original draft preparation, S.Y.; investigation, S.H.; writing—review and editing and visualization, Y.-M.Y.; supervision, review, and edit, S.K. All authors have read and agreed to the published version of the manuscript.

Funding: We acknowledge the financial support of the National Research Foundation under "Next Generation Carbon Upcycling Project" (Project No. 2017M1A2A2042517) of the Ministry of Science and ICT, Republic of Korea. This research was also supported by the Korea Ministry of Environment as part of the Waste to Energy-Recycling Human Resource Development Project (YL-WE-19-002).

Institutional Review Board Statement: Not applicable.

Informed Consent Statement: Not applicable.

Data Availability Statement: Not applicable.

Conflicts of Interest: The authors declare no conflict of interest.

Abbreviations

Full Name	Abbreviation	Unit
Anaerobic digestion	AD	
Carbon-nanotube hollow-fiber media	CHM	
Chemical oxygen demand	COD	mg COD/L
Confocal laser scanning microscopy	CLSM	
Direct interspecies electron transfer	DIET	
interspecies electron transfer	IET	
Methane production rate	MPR	
Operational taxonomic units	OTUs	
Organic loading rate	OLR	g COD/L/day
Polymeric hollow-fiber media	PHM	

References

1. World Biogas Association. Available online: https://www.worldbiogasassociation.org/wp-content/uploads/2019/07/WBA-globalreport-56ppa4_digital.pdf (accessed on 27 December 2020).
2. Zhang, P.; Yan, F.; Du, C. A comprehensive analysis of energy management strategies for hybrid electric vehicles based on bibliometrics. *Renew. Sust. Energ. Rev.* **2015**, *48*, 88–104. [CrossRef]
3. Available online: https://www.fortunebusinessinsights.com/industry-reports/biogas-market-100910 (accessed on 27 December 2020).
4. Rajagopal, R.; Massé, D.I.; Singh, G. A critical review on inhibition of anaerobic digestion process by excess ammonia. *Bioresour. Technol.* **2013**, *143*, 632–641. [CrossRef] [PubMed]
5. Sposob, M.; Moon, H.S.; Lee, D.; Kim, T.H.; Yun, Y.M. Comprehensive analysis of the microbial communities and operational parameters of two full-scale anaerobic digestion plants treating food waste in South Korea: Seasonal variation and effect of ammonia. *J. Hazard. Mater.* **2020**, *398*, 122975. [CrossRef]
6. Baek, G.; Jung, H.; Kim, J.; Lee, C. A long-term study on the effect of magnetite supplementation in continuous anaerobic digestion of dairy effluent–magnetic separation and recycling of magnetite. *Bioresour. Technol.* **2017**, *241*, 830–840. [CrossRef]
7. Baek, G.; Shi, L.; Rossi, R.; Logan, B.E. The effect of high applied voltages on bioanodes of microbial electrolysis cells in the presence of chlorides. *Chem. Eng. J.* **2021**, *405*, 126742. [CrossRef]
8. Chen, S.; Rotaru, A.-E.; Shrestha, P.M.; Malvankar, N.S.; Liu, F.; Fan, W.; Nevin, K.P.; Lovley, D.R. Promoting Interspecies Electron Transfer with Biochar. *Sci. Rep.* **2014**, 5019. [CrossRef]
9. Summers, Z.M.; Fogarty, H.E.; Leang, C.; Franks, A.E.; Malvankar, N.S.; Lovley, D.R. Direct Exchange of Electrons Within Aggregates of an Evolved Syntrophic Coculture of Anaerobic Bacteria. *Science* **2010**, *330*, 1413–1415. [CrossRef]
10. Zhao, Z.; Zhang, Y.; Holmes, D.E.; Dang, Y.; Woodard, T.L.; Nevin, K.P.; Lovley, D.R. Potential enhancement of direct interspecies electron transfer for syntrophic metabolism of propionate and butyrate with biochar in up-flow anaerobic sludge blanket reactors. *Bioresour. Technol.* **2016**, *209*, 148–156. [CrossRef]
11. Yee, M.O.; Rotaru, A.E. Extracellular electron uptake in Methanosarcinales is independent of multiheme c-type cytochromes. *Sci. Rep.* **2020**, *10*, 1–12. [CrossRef]
12. Kato, S.; Hashimoto, K.; Watanabe, K. Microbial interspecies electron transfer via electric currents through conductive minerals. *Proc. Natl. Acad. Sci. USA* **2012**, *109*, 10042–10046. [CrossRef] [PubMed]
13. Lee, J.-Y.; Lee, S.-H.; Park, H.-D. Enrichment of specific electroactive microorganisms and enhancement of methane production by adding granular activated carbon in anaerobic reactors. *Bioresour. Technol.* **2016**, *205*, 205–212. [CrossRef]

14. Lekawa-Raus, A.; Patmore, J.; Kurzepa, L.; Bulmer, J.; Koziol, K. Electrical Properties of Carbon Nanotube Based Fibers and Their Future Use in Electrical Wiring. *Adv. Funct. Mater.* **2014**, *24*, 3661–3682. [CrossRef]
15. Wei, G.; Yu, H.; Quan, X.; Chen, S.; Zhao, H.; Fan, X. Constructing All Carbon Nanotube Hollow Fiber Membranes with Improved Performance in Separation and Antifouling for Water Treatment. *Environ. Sci. Technol.* **2014**, *48*, 8062–8068. [CrossRef]
16. Matsumoto, K.; Uejima, H.; Iwasaki, T.; Sano, Y.; Sumino, H. Studies on regenerated protein fibers. III. Production of regenerated silk fibroin fiber by the self-dialyzing wet spinning method. *J. Appl. Polym. Sci.* **1996**, *60*, 503–511. [CrossRef]
17. Gilcreas, F.W. Standard methods for the examination of water and waste water. *Am. J. Public Health Nation's Health* **1966**, *56*, 387–388. [CrossRef]
18. Viggi, C.C.; Rossetti, S.; Fazi, S.; Paiano, P.; Majone, M.; Aulenta, F. Magnetite Particles Triggering a Faster and More Robust Syntrophic Pathway of Methanogenic Propionate Degradation. *Environ. Sci. Technol.* **2014**, *48*, 7536–7543. [CrossRef]
19. Yun, Y.M.; Sung, S.; Shin, H.S.; Han, J.I.; Kim, H.W.; Kim, D.H. Producing desulfurized biogas through removal of sulfate in the first-stage of a two-stage anaerobic digestion. *Biotechnol. Bioeng.* **2017**, *114*, 970–979. [CrossRef]
20. Regueiro, L.; Veiga, P.; Figueroa, M.; Alonso-Gutierrez, J.; Stams, A.J.M.; Lema, J.M.; Carballa, M. Relationship between microbial activity and microbial community structure in six full-scale anaerobic digesters. *Microbiol. Res.* **2012**, *167*, 581–589. [CrossRef] [PubMed]
21. Hawkes, F.R.; Dinsdale, R.; Hawkes, D.L.; Hussy, I. Sustainable fermentative hydrogen production: Challenges for process optimisation. *Int. J. Hydrog. Energy* **2002**, *27*, 1339–1347. [CrossRef]
22. Xia, Y.; Massé, D.I.; McAllister, T.A.; Kong, Y.; Seviour, R.; Beaulieu, C. Identity and diversity of archaeal communities during anaerobic co-digestion of chicken feathers and other animal wastes. *Bioresour. Technol.* **2012**, *110*, 111–119. [CrossRef] [PubMed]
23. Hu, X.; Du, H.; Ren, C.; Xu, Y. Illuminating Anaerobic Microbial Community and Cooccurrence Patterns across a Quality Gradient in Chinese Liquor Fermentation Pit Muds. *Appl. Environ. Microbiol.* **2016**, *82*, 2506–2515. [CrossRef]
24. Ledezma, P.; Lu, Y.; Freguia, S. Electroactive haloalkaliphiles exhibit exceptional tolerance to free ammonia. *FEMS Microbiol. Lett.* **2017**, *365*, fnx260. [CrossRef] [PubMed]
25. Moscoviz, R.; de Fouchécour, F.; Santa-Catalina, G.; Bernet, N.; Trably, E. Cooperative growth of Geobacter sulfurreducens and Clostridium pasteurianum with subsequent metabolic shift in glycerol fermentation. *Sci. Rep.* **2017**, *7*, 44334. [CrossRef] [PubMed]
26. Salvador, A.F.; Martins, G.; Melle-Franco, M.; Serpa, R.; Stams, A.J.M.; Cavaleiro, A.J.; Pereira, M.A.; Alves, M.M. Carbon nanotubes accelerate methane production in pure cultures of methanogens and in a syntrophic coculture. *Environ. Microbiol.* **2017**, *19*, 2727–2739. [CrossRef]
27. Dang, Y.; Holmes, D.E.; Zhao, Z.; Woodard, T.L.; Zhang, Y.; Sun, D.; Wang, L.-Y.; Nevin, K.P.; Lovley, D.R. Enhancing anaerobic digestion of complex organic waste with carbon-based conductive materials. *Bioresour. Technol.* **2016**, *220*, 516–522. [CrossRef] [PubMed]
28. Diaz, C.; Baena, S.; Fardeau, M.-L.; Patel, B.K.C. Aminiphilus circumscriptus gen. nov., sp. nov., an anaerobic amino-acid-degrading bacterium from an upflow anaerobic sludge reactor. *Int. J. Syst. Evol. Microbiol.* **2007**, *57*, 1914–1918. [CrossRef]
29. Li, Y.; Zhang, Y.; Yang, Y.; Quan, X.; Zhao, Z. Potentially direct interspecies electron transfer of methanogenesis for syntrophic metabolism under sulfate reducing conditions with stainless steel. *Bioresour. Technol.* **2017**, *234*, 303–309. [CrossRef]
30. Liu, F.; Rotaru, A.E.; Shrestha, P.M.; Malvankar, N.S.; Nevin, K.P.; Lovley, D.R. Promoting direct interspecies electron transfer with activated carbon. *Energy Environ. Sci.* **2012**, *5*, 8982–8989. [CrossRef]
31. Kang, S.; Mauter, M.S.; Elimelech, M. Physicochemical Determinants of Multiwalled Carbon Nanotube Bacterial Cytotoxicity. *Environ. Sci. Technol.* **2008**, *42*, 7528–7534. [CrossRef]